ORGANIC LETTERS

2005
Vol. 7, No. 20
4471−4474

Enhanced Small-Molecule Assembly through Directional Intramolecular Forces

Andrew J. Lampkins, Osama Abdul-Rahim, Hengfeng Li, and Ronald K. Castellano*

Department of Chemistry, University of Florida, P.O. Box 117200, Gainesville, Florida 32611-7200

castellano@chem.ufl.edu

Received July 26, 2005

ABSTRACT

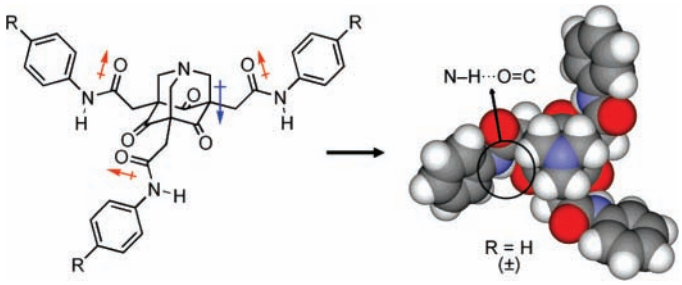

Directional intramolecular interactions play a critical role in the self-assembly of donor-σ-acceptor molecules in solution. Amide functions on the periphery of the tricyclic core stabilize a C_3-symmetric monomer conformation by intramolecular hydrogen bonding and dipole–dipole interactions. The molecules are effective organogelators and show long-range ordering in the bulk.

Directional noncovalent interactions, such as hydrogen bonding and $\pi-\pi$ stacking, underlie self-assembly strategies to control the association and alignment of functional organic molecules in solution wherefrom useful macromolecular properties and architectures emerge.[1,2] We recently demonstrated[3] that suitably functionalized donor-σ-acceptor (D-σ-A) molecules **1**[4] (Figure 1) are prone to self-assemble in solution, thus introducing σ-coupled donor−acceptor interactions[5−7] as complements to traditional forces in the directed self-organization of small molecules.[8] Tribenzyl 1-aza-adamantanetrione **1a**, for example, shows organogelation behavior and the formation of fibrous structures from the gel phase.[3,9]

In this communication we demonstrate how the macromolecular properties and solid-state ordering of D-σ-A molecules can be uniquely modulated by substituents that experience specific intramolecular interactions with the core.

(1) Lehn, J.-M. *Supramolecular Chemistry*; VCH: Weinheim, 1995.
(2) (a) Whitesides, G. M.; Mathias, J. P.; Seto, C. T. *Science* **1991**, *254*, 1312−1319. (b) Lawrence, D. S.; Jiang, T.; Levett, M. *Chem. Rev.* **1995**, *95*, 2229−2260. (c) Hof, F.; Craig, S. L.; Nuckolls, C.; Rebek, J., Jr. *Angew. Chem., Int. Ed.* **2002**, *67*, 8291−8298. (d) Elemans, J. A. A. W.; Rowan, A. E.; Nolte, R. J. M. *J. Mater. Chem.* **2003**, *13*, 2661−2670. (e) Hoeben, F. J. M.; Jonkheijm, P.; Meijer, E. W.; Schenning, A. *Chem. Rev.* **2005**, *105*, 1491−1546.
(3) Li, H.; Homan, E. A.; Lampkins, A. J.; Ghiviriga, I.; Castellano, R. K. *Org. Lett.* **2005**, *7*, 443−446.
(4) For the original synthesis of the 1-aza-adamantanetrione core, see: Risch, N. *J. Chem. Soc., Chem. Commun.* **1983**, 532−533.
(5) Cookson, R. C.; Henstock, J.; Hudec, J. *J. Am. Chem. Soc.* **1966**, *88*, 1060−1062.
(6) (a) Verhoeven, J. W.; Dirkx, I. P.; de Boer, T. J. *Tetrahedron Lett.* **1966**, *7*, 4399−4404. (b) Dekkers, A. W. J.; Verhoeven, J. W.; Speckamp, W. N. *Tetrahedron* **1973**, *29*, 1691−1696. (c) Worrell, C.; Verhoeven, J. W.; Speckamp, W. N. *Tetrahedron* **1974**, *30*, 3525−3531. (d) Pasman, P.; Verhoeven, J. W.; de Boer, T. J. *Tetrahedron* **1976**, *32*, 2827−2830.
(7) (a) Hoffmann, R. *Acc. Chem. Res.* **1971**, *4*, 1−9. (b) Gleiter, R. *Angew. Chem., Int. Ed. Engl.* **1974**, *13*, 696−701. (c) Paddon-Row, M. N. *Acc. Chem. Res.* **1982**, *15*, 245−251.
(8) For the self-assembly of *π-conjugated* donor−acceptor chromophores, see: Yao, S.; Beginn, U.; Gress, T.; Lysetska, M.; Würthner, F. *J. Am. Chem. Soc.* **2004**, *126*, 8336−8348 and references therein.
(9) (a) Terech, P.; Weiss, R. G. *Chem. Rev.* **1997**, *97*, 3133−3159. (b) Abdallah, D. J.; Weiss, R. G. *Adv. Mater.* **2000**, *12*, 1237−1247. (c) Gronwald, O.; Snip, E.; Shinkai, S. *Curr. Opin. Colloid Interface Sci.* **2002**, *7*, 148−156.

10.1021/ol051768x CCC: $30.25
Published on Web 09/03/2005

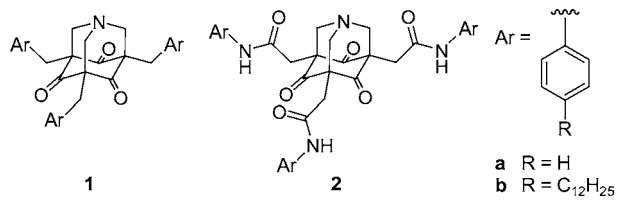

Figure 1. Aryl-functionalized donor-σ-acceptor molecules.

Triamides of the 1-aza-adamantanetriones **2** are introduced that show enhanced aggregation properties relative to **1** and form stable and ordered assemblies in solution, the gel phase, and the bulk. Studies implicate the amide groups in this disparate behavior, but not through their participation in traditional intermolecular hydrogen-bonding interactions. Featured are intramolecular seven-membered ring N−H(amide)···O(ketone) H-bonding and favorable electrostatic interactions between the opposing core and amide dipoles. The effects mutually stabilize (1) a C_3-symmetric conformation of the monomer that is "active" in self-assembly and (2) ground state σ-coupled donor−acceptor interactions at the core. The latter intramolecular "solvation" of the D-σ-A core by peripheral dipolar functional groups appears as a new way to tune the electronic and macromolecular properties of these systems.

The synthesis of the 1-aza-adamantanetrione triamides **2** is outlined in Scheme 1. Bromomethylated phloroglucinol

Scheme 1. Synthesis of Amide-Functionalized 1-Aza-adamantanetriones **2**

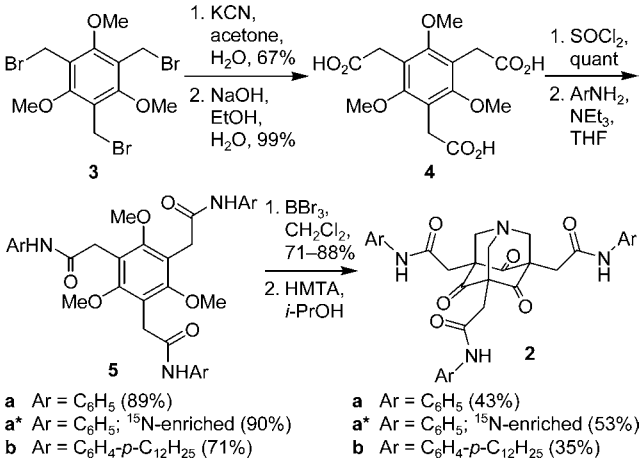

derivative **3**[3] is converted to tricarboxylic acid **4** through benzylic substitution with cyanide followed by base-catalyzed hydrolysis of the nitrile functions. Activation of the triacid and subsequent amide bond formation with an appropriate aniline derivative gives **5**. In addition to aniline (to afford **5a**), ^{15}N-enriched aniline imparts an isotopic probe (**5a***), and *p*-dodecylaniline introduces a solubilizing substituent (**5b**). Deprotection of the core with BBr_3 and cyclization with hexamethylenetetramine (HMTA)[3,4] in 2-propanol at reflux provides tricyclic targets **2**. The moderate yield of the final step is offset by the simple purification of the products that only involves filtration and at most a single recrystallization (for **2b**).

Solubility studies of amides **2** in common organic solvents immediately reveal their unusual solution-phase behavior and propensity for aggregation. Trianilide **2a** is sparingly soluble in most organic solvents, and surprisingly limited improvement comes with even dodecyl (**2b**) substituents on the aromatic rings. This behavior is in contrast to **1b** (Figure 1), which shows good solubility in a broad range of organic solvents at room temperature. Most interesting is the behavior of **2b** in halogenated solvents (e.g., chloroform, carbon tetrachloride, and 1,1,2,2-tetrachloroethane) where it rapidly (in minutes) forms optically clear gels[9] following heating and cooling. For chloroform, the most effectively gelled solvent, complete immobilization of the solution is observed at ~0.5 wt % (the critical gelation concentration) with a sol−gel transition temperature (T_{gel}) of 57 °C, the highest value that we have observed for this class of gelators thus far. Moreover, the chloroform gels of **2b** show no sign of precipitation after months at room temperature. The DMSO gels of **1a** are comparatively less stable,[3] but this difference can only partially be attributed to the additional alkyl chains of **2b**. Derivative **1b** requires both higher concentration (ca. 2 wt %) and lower temperature (−15 °C) for aggregation,[10] with the compound remaining freely soluble in chloroform at room temperature.

Freeze-dried samples of the chloroform gels of **2b** were studied by SEM (Figure 2a,b). Unlike the fibrous morphology of the dried gels of **1a** and many organogelators,[9] here a lamellar architecture is observed that in some regions appears as layered slabs of fairly uniform thickness (200−500 nm, Figure 2a) and in others more typical curved, wrinkled sheets (Figure 2b).[11] X-ray diffraction (XRD) studies (Figure 2c) also reveal this long-range periodic order for the neat (solid) samples of **2b** where an intense low-angle peak is observed at a *d*-spacing of 30.1 Å (001) and two higher-order reflections are found at 15.1 Å (002) and 9.7 Å (003). Also evident is a diffuse band attributable to packing of the alkyl side chains (d = 4.7 Å). Of particular relevance to **2b**, similar layered (smectic) structural order has been characterized for propeller-shaped metallomesogens[12] and for bowl-shaped CTVs and calixarenes.[13,14] Interestingly, both **1a** and **1b**, which lack amide functions, show significantly weaker XRD

(10) At these conditions the mixture is turbid and stable to inversion. The material "melts" sharply at ca. −5 °C upon warming.

(11) For recent examples of gelators that show lamellar architectures, see: (a) Kölbel, M.; Menger, F. M. *Chem. Commun.* **2001**, 275−276. (b) Jung, J. H.; Shinkai, S.; Shimizu, T. *Chem. Eur. J.* **2002**, *8*, 2684−2690. (c) Park, S. M.; Lee, Y. S.; Kim, B. H. *Chem. Commun.* **2003**, 2912−2913. (d) Jang, W.-D.; Aida, T. *Macromolecules* **2003**, *36*, 8461−8469. (e) John, G.; Jung, J. H.; Masuda, M.; Shimizu, T. *Langmuir* **2004**, *20*, 2060−2065. (f) Moreau, J. J. E.; Vellutini, L.; Wong Chi Man, M.; Bied, C.; Dieudonné, P.; Bantignies, J.-L.; Sauvajol, J.-L. *Chem. Eur. J.* **2005**, *11*, 1527−1537. (g) Tanaka, S.; Shirakawa, M.; Kaneko, K.; Takeuchi, M.; Shinkai, S. *Langmuir* **2005**, *21*, 2163−2172.

(12) Zheng, H.; Swager, T. M. *J. Am. Chem. Soc.* **1994**, *116*, 761−762.

(13) Lunkwitz, R.; Tschierske, C.; Diele, S. *J. Mater. Chem.* **1997**, *7*, 2001−2011.

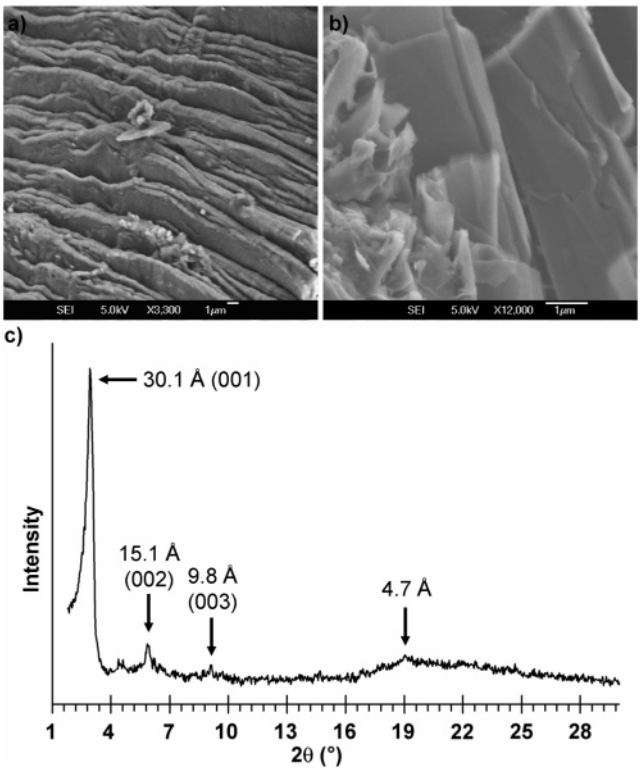

Figure 2. Structural order within amide-functionalized 1-aza-adamantanetriones **2**: (a, b) SEM images of a xerogel formed from freeze-drying the 0.5 wt % chloroform gel of **2b**; (c) X-ray diffraction pattern of neat **2b** at 21 °C.

patterns and numerous Bragg peaks at room temperature for their solids (not shown).

The role of the amide functions in the self-assembly behavior of **2** could be probed through IR and NMR measurements and by computational analysis. The lowest energy conformer[15] of the simplified aza-adamantanetrione core bearing one anilide substituent and two methyl substituents (Figure 3a) displays seven-membered ring H-bonding between the amide NH and the core carbonyl. Also apparent in this conformation is how the dipole of the D-σ-A core and dipole of the peripheral amide are favorably opposed.[16] Transposing this lowest energy single arm conformation to all three arms of **2** creates the C_3-symmetric (and racemic), propeller-shaped[17] conformer of **2a** shown as an energy-minimized space-filling model (Figure 3b). Superimposition shows that this conformation[18,19] is pseudoisosteric with the predicted low-energy structure of **1a** (orange bonds, Figure 3c) previously implicated in self-assembly.[3] Direct evidence

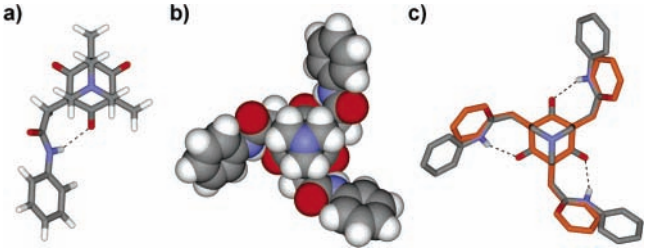

Figure 3. Computational analysis:[15] (a) top view of the low-energy conformation of a simplified version of **2a**; (b) the "active" self-assembling conformation of **2a** based on computation and spectroscopic studies (top view as a space-filling representation); (c) the superimposed energy-minimized structures of **1a** (orange)[3] and **2a**; hydrogen atoms have been omitted for clarity. Hydrogen bonding is shown by the dashed lines. All molecules are racemic.

that a *symmetric* H-bonded conformation of triamide **2** exists as the "active" self-assembled conformer follows through spectroscopic studies in solution and the solid state.

To assess H-bonding within **2** we performed IR and NMR studies with **2a**,**b** and commercially available *N*-phenylacetamide **6** (Figure 4a, inset).[20] The model shows predictable amide behavior in solution (solid line); at 0.2 M in $CHCl_3$ a sharp absorption is observed at 3440 cm^{-1} that represents the solvent-associated ("free") NH stretch, while a broad absorption is detectable at 3325 cm^{-1} arising from intermolecular amide−amide H-bonding.[21,22] The latter peak grows in at higher concentrations and is not seen below ca. 10 mM. The IR spectrum of **2b** (Figure 4a, dashed line) shows a *single*, moderately sharp NH absorption at 3360 cm^{-1} in $CHCl_3$ at 3.4 mM (0.25 wt %).[23] The shift of the amide NH absorption of **2b** to this unique frequency is consistent with seven-membered ring H-bonding involving the amide NH and ketone carbonyl group; similar frequencies are reported for intramolecularly H-bonded γ-ketoamides[24] (ν N−H···O = 3335−3380 cm^{-1} and ν N−H_{free} = 3440

(14) Dodecyl **2b** does exhibit an endothermic phase transition at ca. 185 °C (DSC) where a viscous, birefringent texture is also observed by polarized light microscopy. The phase behavior of both **2a** and **2b** is currently being explored.

(15) See the Supporting Information for computational details.

(16) The related H-bonded substituent conformation that inverts the amide group (not shown) is calculated to be 3.7 kcal mol^{-1} higher in energy (at the HF/6-31G* level).

(17) Mislow, K. *Acc. Chem. Res.* **1976**, *9*, 26−33.

(18) The C_1-symmetric conformer with two amides H-bonded to a single carbonyl suffers from steric repulsion between the aromatic rings.

(19) Opposition of the peripheral amide dipoles and donor-σ-acceptor core dipole reduces the molecular dipole moment (at the HF/6-31G* level **1a** = 4.1 D, **2a** = 3.4 D) but *stabilizes* the σ-coupled donor−acceptor interactions at the core based on the large *downfield* ^{1}H NMR chemical shift of the *core* N-α-CH_2 protons[3] of **2** relative to **1** ($\Delta\delta$ ~0.5 ppm) in halogenated and polar solvents.

(20) That the amides of **2** and **6** are electronically comparable comes through NMR studies of the monomeric species in DMSO-d_6 (ca. 10 mM): NH ^{1}H NMR chemical shift, **2a** = 10.0 ppm, **6** = 9.8 ppm; amide C=O ^{13}C NMR chemical shift, **2a** = 168.0 ppm, **6** = 168.4 ppm.

(21) In the bulk (Nujol), exclusive intermolecular H-bonding is observed for **6** given as a broad NH absorption at 3288 cm^{-1}. This is consistent with the X-ray crystal structure of **6** (CSD code ACANIL01), which shows intermolecular hydrogen bonding with an N···O distance of 2.91 Å.

(22) For detailed studies of intramolecular hydrogen-bonding phenomena, see: (a) Gellman, S. H.; Dado, G. P.; Liang, G.-B.; Adams, B. R. *J. Am. Chem. Soc.* **1991**, *113*, 1164−1173. (b) Dado, G. P.; Gellman, S. H. *J. Am. Chem. Soc.* **1993**, *115*, 4228−4245.

(23) The NH stretch frequency and NH ^{1}H NMR chemical shift (vide infra) are concentration-independent within the 3-fold concentration range permitted by instrument sensitivity at lower concentrations and extensive aggregation at higher concentrations. The peak at 3360 cm^{-1} is observed as the sole band in the NH region in the bulk (Nujol) and the gel phase (at 0.50 wt % by ATR-IR spectroscopy).

(24) (a) Chiron, R.; Maisonneuve, P.; Graff, Y. *C. R. Acad. Sci. Paris, Ser. C* **1973**, *276*, 105−108. (b) Chiron, R.; Graff, Y. *Spectrochim. Acta, Part A* **1976**, *32*, 1303−1310.

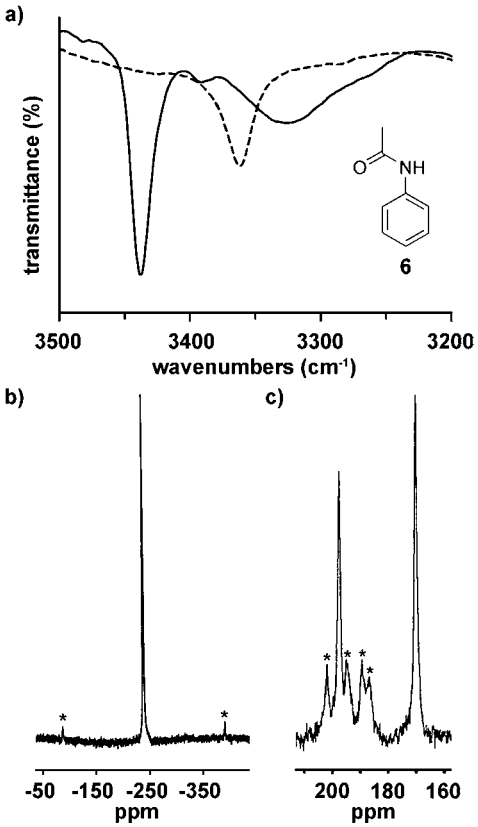

Figure 4. (a) The IR spectrum of **6** at 0.2 M in chloroform (solid line) shows both a "free" amide NH stretch (3440 cm^{-1}) and evidence for intermolecular H-bonding (3325 cm^{-1}); the spectrum of **2b** at 3.4 mM (0.25 wt %; dashed line) shows exclusive intramolecular H-bonding (3360 cm^{-1}); the ^{15}N (b) and ^{13}C (c) CPMAS NMR spectra of **2a*** reveal a symmetrical monomer in the solid state. Starred peaks represent sidebands.

cm^{-1} (at 1 mM in CCl_4)). That no "free" NH stretch is detectable for **2b** in dilute solution (to the detection limit, ~0.10 wt %) demonstrates that intramolecular H-bonding is uniquely present, presumably coupled with monomer aggregation.

The IR studies are qualitatively supported by NMR measurements.[22] Not unexpectedly, the ^1H NMR spectra of **2b** in deuterated halogenated solvents are broadened, indicative of extensive aggregation. This is even the case for **2b** in $CDCl_3$ at low concentration (2 mM) and elevated temperature (323 K), although the amide NH remains a fairly sharp singlet at 7.62 ppm (downfield of TMS). VT NMR measurements of **2b** at 13 mM in the higher boiling $C_2D_2Cl_4$ confirm a very small temperature dependence for the amide proton (7.60−7.44 ppm from 298 to 398 K; $\Delta\delta/\Delta T = -1.6$ ppb/K), consistent with intramolecular H-bonding.[22,25] For comparison, the −NH shift of **6** in $C_2D_2Cl_4$ at 298 K and the amide molar equivalent concentration of 39 mM is 7.1 ppm. Dilution experiments for **6** confirm that this is near the upfield limiting chemical shift of 7.0 ppm that represents the monomeric species in this solvent.[26] That the amide chemical shift of **2b** remains downfield of this value at the highest accessible NMR temperature reflects stable aggregates in solution and exclusive intramolecular H-bonding to the core.

Final evidence for the C_3-symmetric conformation proposed for **2** (Figure 3b) comes through solid-state NMR studies performed with ^{15}N-enriched **2a*** (Scheme 1). The ^{15}N CPMAS NMR spectrum (Figure 4b) shows one sharp peak for the three equivalent amide nitrogens at −241.9 ppm, while the ^{13}C CPMAS NMR spectrum (Figure 4c) reveals two carbonyl resonances, one from the amides (169.5 ppm) and one from the three equivalent core ketones (197.0 ppm).[27] These results importantly contrast with the previously obtained ^{13}C CPMAS NMR data for **1a**, which revealed multiple ^{13}C resonances and a loss of symmetry in the solid state.[3] Taken together with the powder XRD results, **2** shows both long-range and local order in the bulk. With these data in hand and ready access to derivatives through synthesis (Scheme 1), we are undertaking detailed structural investigations to elucidate a general model for the packing of **2**.[13,28]

In summary, amide-functionalized D-σ-A molecules **2** show enhanced self-assembly properties in solution and significantly more order in the solid state relative to congeners **1**. Spectroscopic and computational studies implicate a unique interplay between the amide functions and the donor-σ-acceptor core in this behavior, where intramolecular hydrogen bonding and dipolar interactions stabilize the C_3-symmetric conformation of the monomer required for self-assembly. We are currently exploring in more detail how neighboring dipolar functional groups can tune the σ-coupled donor−acceptor interactions in these molecules toward further controlling their macromolecular behavior in solution.

Acknowledgment. We are grateful to the University of Florida for financial support. A.J.L. is a UF Alumni Graduate Fellow. We thank Dr. Kerry Siebein of the UF Major Analytical Instrumentation Center (UF MAIC) for the SEM measurements, Dana Horoszewski and Prof. Colin Nuckolls (Columbia University) for assistance with the X-ray diffraction, Prof. Joanna Long for the solid-state NMR measurements, and Dr. Phil Britt of the Center for Nanophase Materials Sciences at Oak Ridge National Laboratories for insightful discussions.

Supporting Information Available: Synthetic details and characterization data, computational protocols, additional XRD data, and relevant NMR data. This material is available free of charge via the Internet at http://pubs.acs.org.

OL051768X

(25) Stevens, E. S.; Sugawara, N.; Bonora, G. M.; Toniolo, C. *J. Am. Chem. Soc.* **1980**, *102*, 7048−7050 and references therein.

(26) Luo, W. C.; Chen, J. S. *Z. Phys. Chem.* (*Muenchen*) **2001**, *215*, 447−459.

(27) For comparison, ^{15}N-enriched **6** shows single ^{15}N and ^{13}C (carbonyl carbon) resonances at −244.1 and 171.4 ppm, respectively.

(28) (a) Malthête, J.; Collet, A. *J. Am. Chem. Soc.* **1987**, *109*, 7544−7545. (b) Serrette, A. G.; Lai, C. K.; Swager, T. M. *Chem. Mater.* **1994**, *6*, 2252−2268. (c) Sawamura, M.; Kawai, K.; Matsuo, Y.; Kanie, K.; Kato, T.; Nakamura, E. *Nature* **2002**, *419*, 702−705.